



Chic-Marker: Fashionably Fusing Fiducial Markers into Apparel and Accessories

Rong-Hao Liang

Eindhoven University of Technology
Eindhoven, The Netherlands
r.liang@tue.nl

Hannah van Iterson

Eindhoven University of Technology
Eindhoven, The Netherlands
h.c.v.iterson@tue.nl

Holly Krueger

Eindhoven University of Technology
Eindhoven, The Netherlands
h.l.krueger@tue.nl

Marina Toeters

Eindhoven University of Technology
Eindhoven, The Netherlands
m.j.toeters@tue.nl

Loe Feijs

Eindhoven University of Technology
Eindhoven, The Netherlands
r.liang@tue.nl



Figure 1: *Red Herring* is a poncho adorned with the timeless Pied-de-poule pattern with AprilTag36h10 fiducial markers. This garment offers a stylish appearance and enables posture tracking and garment identification.

ABSTRACT

This paper proposes Chic-Marker, a fashionable approach to integrating square fiducial markers into apparel and accessories. While square fiducial markers have found widespread use in industrial and entertainment sectors for precise object identification and tracking, their integration into daily wearable items has been limited due to their conspicuous appearance. Previous efforts to conceal these

markers using infrared-based methods have encountered obstacles, often requiring specialized equipment and lighting conditions. In this study, we propose a fresh perspective by embedding the markers within the timeless Pied-de-poule pattern, enhancing their visibility for tracking purposes and their fashion appeal. We use computational tools to design and manufacture functional garments using sublimation printing and traditional handcrafting techniques. Through rigorous technical evaluation and exploratory making, we analyze the characteristics of these markers and explore their material potential, offering valuable insights and guidelines for their seamless integration into future wearable applications.



This work is licensed under a Creative Commons Attribution International 4.0 License.

CCS CONCEPTS

- Human-centered computing → User interface toolkits; Ubiquitous and mobile computing systems and tools.

KEYWORDS

Fiducial markers, garments, wearables, sublimation printing, fashion technology, computer vision

ACM Reference Format:

Rong-Hao Liang, Hannah van Iterson, Holly Krueger, Marina Toeters, and Loe Feijs. 2024. Chic-Marker: Fashionably Fusing Fiducial Markers into Apparel and Accessories. In *ACM Symposium on Computational Fabrication (SCF '24), July 07–10, 2024, Aarhus, Denmark*. ACM, New York, NY, USA, 15 pages. <https://doi.org/10.1145/3639473.3665790>

1 INTRODUCTION

Fiducial markers [Garrido-Jurado et al. 2014; Kalaitzakis et al. 2021; Olson 2011] are crucial in precise object identification and localization without requiring prior knowledge or training. They are extensively utilized in industrial sectors, particularly in robotics and augmented reality applications, as well as in human-computer interaction. Moreover, the entertainment industry employs these markers as wearables for motion capture [Chen et al. 2021], notably in filmmaking.

Among a universe of fiducial markers, monochromatic square markers, such as AprilTag [Olson 2011; Wang and Olson 2016] and ArUco [Garrido-Jurado et al. 2014; Romero-Ramirez et al. 2018] markers, stand out as the most efficient in terms of 3D position and orientation tracking efficiency and ID encoding. They remain state-of-the-art for marker-based tracking applications [Kalaitzakis et al. 2021]. However, their appearance is perceived as visually obtrusive, so these markers are seldom incorporated into everyday apparel and accessories.

Previous works have utilized infrared ink or filaments (e.g., [Dogan et al. 2022; Kim et al. 2016; Willis et al. 2013]) to make these fiducial tags less visually obtrusive to integrate these markers into invisible physical artifacts for everyday applications. However, decoding these tags requires an infrared imaging module sensitive to environmental conditions or specific illumination to increase the signal-to-noise ratio (e.g., [Dogan et al. 2023]), limiting the availability of the invisible approach in the context of daily applications. Prior research has explored markers in various shapes [Getschmann and Echtler 2021; Yu et al. 2020] and colors [DeGol et al. 2017] to make them less obtrusive and more aesthetically appealing. However, these alternative shapes are less efficient and effective than square markers in object identification and location tracking tasks [Kalaitzakis et al. 2021].

This paper presents a research-through-design [Zimmerman et al. 2007] exploration that takes a fresh perspective, turning the square markers into a fashion opportunity. Instead of hiding the markers, we meticulously integrate them into the timeless Pied-de-poule pattern to allow for reliable tracking using an off-the-shelf camera and increase these square markers' fashion and aesthetic potential. We name this approach *Chic-Marker*.

Figure 1 presents *Red Herring*, a garment that merges fashion with fiducial marker technology. This unique piece blends square fiducial markers with a striking red herring motif and classic Pied-de-poule patterns, resulting in a fashionable design. The fabric incorporates hundreds of AprilTag-36h10 fiducial markers, allowing conventional camera systems to track the wearer's posture. Beyond its visual appeal, the garment offers an interactive experience where

each marker unlocks personal digital surprises through a camera. This garment challenges norms and sparks curiosity, paving the way for further discussion and debate on fashion-driven technology.

Figure 2 shows more examples that feature a variety of Pied-de-poule patterns interwoven with AprilTag-36h11 fiducial markers, including a tube dress (Figure 2a), which is a form-fitting garment that contours to the body's curves; a sleeveless jogging shirt (Figure 2b), which provides breathability and freedom of movement for runners; a reusable shopping bag (Figure 2c), which is a sustainable alternative to single-use plastic bags; and, a handbag (Figure 2d), which is a stylish and functional accessory designed to add a fashionable touch to any outfit. All examples support precise garment identification and tracking. The IDs of successfully detected markers and their relative locations and orientations toward the center of the camera tracking plane are obtained with measurements in real-world units (e.g., cm), allowing for a camera system to track the wearer's posture and the object's movement through a partial observation when at least one marker is detected.

Figure 3 illustrates the computational fabrication process. The pattern is generated and printed on a sublimation transfer paper using a generative algorithm and an inject printer. The counterpart polyester fabric layers are also precisely cut using a laser cutter. Fiducial markers are then heat-transferred onto the polyester fabrics, which are carefully assembled by a fashion designer using a sewing machine. This workflow is seamlessly integrated with the designer's existing garment-making process.

The main contribution of this paper lies in the methodology that harnesses computational tools, digital fabrication, and craftsmanship to unlock the digitalization potential of functional garments. In the subsequent sections, we delve into related work in Section 2, introduce our Chic-Marker approach in Section 3, explore the characteristics and qualities of these fiducial markers through hands-on experimentation in Section 4, discuss implications for future marker integration in wearable applications in Section 5, and conclude the paper in Section 6.

2 RELATED WORK

2.1 Fiducial Markers for Object Identification and Tracking

Fiducial markers are computer-readable visual tags that offer practical ways of enriching the physical world with digital information. Unlike embedded electronic tags like RFID [Want et al. 1999], printed fiducial markers are more practical and hold significant potential for precise 3D localization [Wang and Olson 2016]. Consequently, they are extensively employed in Robot Operating Systems (ROS) for tasks such as unmanned aircraft landing [Sani and Karimian 2017; Wubben et al. 2019] and object tracking [Sugiura et al. 2010; Wang and Olson 2016], as well as in human-centered applications like augmented reality (AR) [Billinghurst et al. 2001; Wu et al. 2017] and motion capturing [Chen et al. 2021]. While a markerless approach such as SLAM (Simultaneous Localization and Mapping [Fuentes-Pacheco et al. 2015]) and SIFT (Scale Invariant Feature Transform [Lowe 2004]) can also be utilized in ROS and AR, marker-based tracking remains simpler, more robust, and provides a perspective to reliably encode data in its payload, inviting walk-up-and-use as it does not necessitate prior training.



Figure 2: Examples that featuring a variety of Pied-de-poule pattern interwoven with AprilTag36h11 fiducial markers: a) a tube dress; b) a sleeveless jogging shirt; c) a reusable shopping bag; d) a handbag. The outlined camera view also shows the fiducial markers printed on these examples were successfully recognized and tracked by OpenCV.

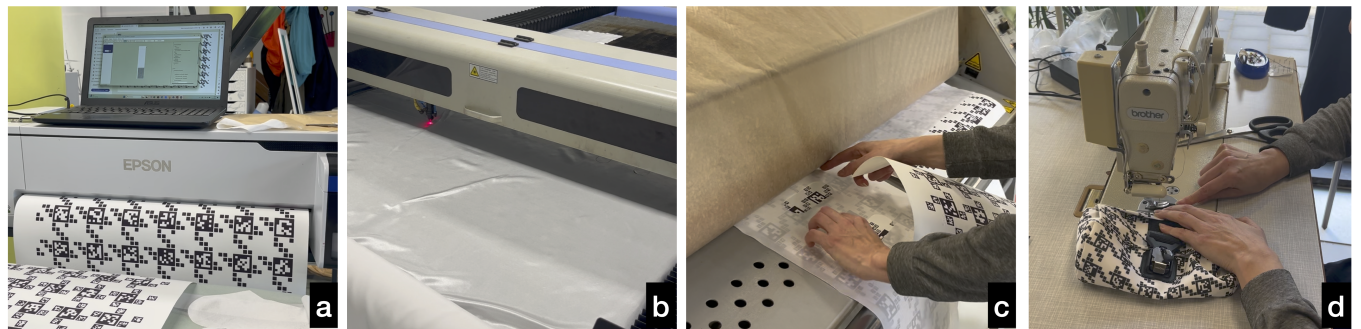


Figure 3: Fabrication process: a) A pattern is printed using a sublimation printer; b) Fabric layers are precisely cut using a laser cutter; c) Markers are heat-transferred onto the fabrics; d) The fabric is assembled using a sewing machine.

Among a universe of fiducial markers, three state-of-the-art options widely used for object identification and tracking, as well as

in AR and ROS applications, are ARTag [Fiala 2005, 2009], AprilTag [Olson 2011; Wang and Olson 2016], and ArUco [Garrido-Jurado et al. 2014; Romero-Ramirez et al. 2018]. They are all square, monochromatic markers featuring a payload matrix that supports

error correction, and they are either open-source or offer a ROS implementation. Kalaitzakis et al. [Kalaitzakis et al. 2021] evaluated the performance of these three types of markers and concluded that these three markers are comparable and all valid for identifying and tracking location and orientation. AprilTag excels in orientation tracking, while ArUco is superior in distance estimation and motion blur handling, and is generally less computationally expensive than the other two.

2.2 Designing Unobtrusive Fiducial Markers

Previous research also investigated the integration of fiducial markers into garments. Häkkilä et al. [Häkkilä et al. 2017] suggest that visual design is very important for acceptability, and a user's personal style largely dictates their preference for the concept and willingness to wear the garment, as well as the role of the user in the markers' appearance. However, Mäkelä et al. [Mäkelä et al. 2007] also found that those fiducial markers were perceived as mathematical and unaesthetic.

HCI researchers have explored methods to seamlessly integrate fiducial markers into artifacts by utilizing infrared (IR) inks and filaments. HideOut [Willis et al. 2013] creates hidden tracking markers by applying IR-absorbing ink with a laser-cut mask on paper. MiniStudio [Kim et al. 2016] employs IR-reflective fiducial markers using silk-screen printing with white ink on a white reflective sticker. InfraredTags [Dogan et al. 2022] allows customization by utilizing 3D printing of IR-absorbing filament, making markers imperceptible by covering them with an opaque IR-passing material. BrightMarker [Dogan et al. 2023] enhances the signal-to-noise ratio by incorporating IR fluorescence illumination. However, decoding these IR tags necessitates an infrared imaging module sensitive to environmental conditions or specific illumination, thus limiting the availability of the invisible approach in daily applications. Another approach involves specific materials such as AirCode [Li et al. 2017] and Terahertz imaging devices like Infrastructs [Willis and Wilson 2013], which are unsuitable for garment tracking.

Previous research has explored fiducial markers in non-square forms, such as circles [Bergamasco et al. 2016, 2011; Calvet et al. 2016; Naimark and Foxlin 2002], custom shapes [Yu et al. 2020], unconventional appearances [Getschmann and Echtler 2021; Kaltenbrunner and Bencina 2007], and colors [DeGol et al. 2017], aiming to make them less obtrusive and more aesthetically appealing. However, while these alternative options may offer benefits in some aspects, such as improved handling of occlusions and graceful performance degradation when tracking fails, they are less efficient and effective than square markers in some key aspects including tracking efficiency, ID encoding, and fault-tolerance [Kalaitzakis et al. 2021]. Overall, square-shaped markers remain reliable and versatile options for marker-based applications.

2.3 Pied-de-poule Patterns

Pied-de-poule, or Houndstooth, was introduced to fashion by the Prince of Wales (Edward VII) in the 1930s and haute couture by Dior in the 1950s. The oldest known garment made of Pied-de-poule fabric is the Gerum cloak found in Sweden, which has been radiocarbon dated to 360–100 BC, the pre-Roman Iron Age [Frei 2009]. It is a special weaving pattern obtained by alternating black

and white bands in the warp and the weft. With a twill binding (e.g., two over, two under), the Pied-de-poule pattern emerges.

Pied-de-poule can be described as a tessellation obtained by translating interlocking black and white tiles, as shown in Figure 4. It is not just one pattern but a family of Pied-de-poule patterns that Feijs' [Feijs 2012] formula can describe:

$a_{\{ij\}} = (i - j) \% 2N < N ? i \% 4N < 2N : j \% 4N < 2N$

where i counts warp yarns (which go vertically), j counts weft yarns (which run horizontally), and the integer $N > 0$. The $N = 1$ case is Puppytooth (Figure 4a). Moreover, there is a limit case when N approaches infinity (Figure 4d), although this cannot be woven, it can be printed or laser-cut.

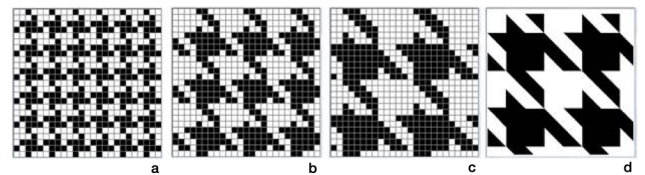


Figure 4: Pied-de-poule patterns: a) $N=1$; b) $N=2$; c) $N=3$; d) $N=\infty$.

While the classic Pied-de-poule pattern has ancient origins, the same design is recycled repeatedly in different contexts, garment cuts, and combinations. Pied-de-poule is frequently used in haute couture, prêt-à-porter, and mass-produced fashion. Pied-de-poule is used more in designs for women than for men. Usually, the pattern appears in black and white, yet it can also be found in more subdued color variations. Celebrities such as Lady Gaga, the Princess of Wales, and the queens of Belgium and the Netherlands frequently appear in flamboyant Pied-de-poule coats, further cementing its status as a timeless fashion statement.

3 CHIC-MARKER

This section outlines our Chic-Marker approach to integrating square fiducial markers into Pied-de-poule patterns. We introduce the design considerations and then propose a family of variants. Following this, we conduct a technical evaluation to explore the implications of marker design on their recognition and tracking performance. Additionally, we introduce material exploration on sublimation printing fiducial markers on fabrics.

3.1 Design Principles

Before introducing the design, we need to address three primary design considerations.

- **P1. Optimizing Object Identification and Tracking.** Our exploration begins with black and white colors, which help maximize contrast, making it easier for computer vision systems to distinguish fiducial markers from their surroundings. Maintaining the square shape and matrix geometry of fiducial markers also retains their recognition and decoding capability. Moreover, enlarging the fiducial markers as much as possible improves their detectability, especially from a distance or under varying lighting conditions.

- **P2. Efficient Use of IDs.** A greater number of unique markers is essential to accommodate larger garments. Therefore, optimizing ID utilization enables the creation of larger garments capable of supporting human-size applications or facilitating higher marker density deployments to manage deformation issues effectively. Moreover, it provides a broader perspective for tracking multiple objects simultaneously.
- **P3. Balancing Aesthetic and Performance.** Designing applications where visual appeal is as important as functionality involves ensuring that the appearance of Pied-de-poule, a classic pattern known for its elegance and sophistication, is preserved. This adds a touch of style to the markers without compromising their tracking performance.

By striking the right balance between aesthetics and performance, human-scale applications can achieve visual appeal and accurate object identification and tracking capabilities. This enhances user experience and satisfaction, ensuring the application meets functional and aesthetic requirements.

3.2 Integrating Fiducial Markers into Pied-de-poule Patterns

Figure 5 illustrates our design approach for a 16x16 pattern, integrating a 2x2 tile of 8x8 Pied-de-poule ($N=2$) units, and incorporates several key strategies. Firstly, we substitute each pixel of a Pied-de-poule pattern with a unique marker that can be identified and tracked individually, as shown in Figure 5a. To optimize the identification and tracking of an object on which the pattern is applied, we replace the 4x4 grid of markers with a 4-times larger marker to maximize marker visibility, as shown in Figure 5b, ensuring clearer recognition and tracking at a longer distance (**P1**). Since the ID and sizes of the large and small markers are known, the two classes of markers can be detected using separate marker detectors configured with different marker size settings to ensure the validity of location and orientation tracking. Lastly, to optimize ID space usage, smaller markers within the pattern can be repurposed as decorative elements, as shown in Figure 5c, while preserving aesthetic appeal and functionality (**P2**).

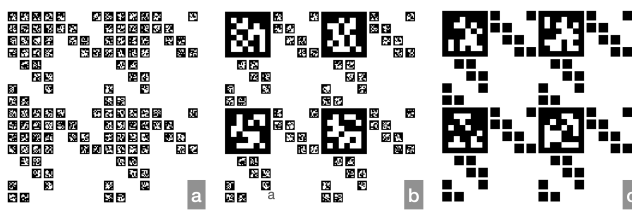


Figure 5: Designing with $N=2$ Pied-de-poule units: a) Replacing each pixel with an AprilTag36h11 marker; b) maximizing the marker's visibility using a 4x larger pattern; c) freeing up the ID space by repurposing smaller markers as decorative elements, such as squares.

In Figure 5b, the recognition and tracking of the small markers are limited since they are four times smaller than the large ones. Therefore, we explore the $N=1$ Pied-de-poule pattern, namely Puppytooth. Figure 6 illustrates our design approach for a 16x16 pattern,

integrating a 4x4 tile of 4x4 Puppytooth units. Firstly, we substitute each pixel of a Puppytooth pattern with a unique marker that can be identified and tracked individually, as shown in Figure 6a. To optimize the identification and tracking of an object applied to this pattern, we replace the 2x2 grid of markers with a 2-times larger marker to maximize marker visibility, as shown in Figure 6b. In this case, the small markers are only two times smaller than the large ones, making them more detectable when the large markers are detected (**P1**). The Puppytooth pattern also requires fewer IDs than the Pied-de-poule one when covering the same area size (**P2**).

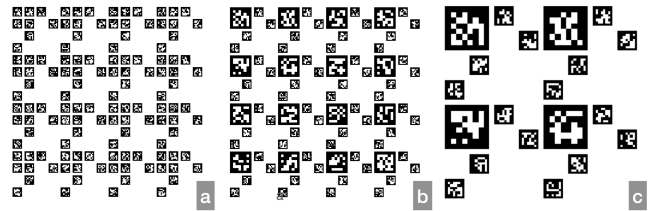


Figure 6: Designing with 4x4 Puppytooth (i.e., $N=1$ Pied-de-poule) units: a) Replacing each pixel with an AprilTag36h11 marker; b) maximizing the marker's visibility using a 2x larger pattern. c) Puppytooth patterns consume fewer IDs than the $N=2$ Pied-de-poule patterns and improve the visibility of the smaller markers.

Since the fiducial tracking algorithm needs to extract the square marker's corners for identification and tracking, having a margin surrounding the marker is necessary. However, while increasing the margin width between visual components enhances the visibility of the markers, it also reduces the overall visual continuity of the pattern as a whole. Figure 7 illustrates 16x16 patterns with the same marker size but different gap distances between the visual components. When the fiducial marker has a fixed width W , increasing the margin width m would result in the size s of a decorator decreasing as $s = (W - (2N - 1) * m) / 2N$ for a Pied-de-poule pattern of N , thus reducing the visual weight of the decorator in an undesirably discrete manner. Therefore, the value of m must be carefully chosen to balance aesthetics and performance (**P3**).

3.3 Analyzing Margin Width's Impact on Marker Tracking

We conducted two technical evaluation sessions to understand how the margin width between the fiducial markers could impact marker tracking.

3.3.1 Session 1. Margin Width vs. Marker Orientation. The first session investigates how the margin width impacts the marker's detection performance on various marker sizes and orientations.

Methods. Figure 8a depicts the experimental setup, comprising a webcam, a turntable on a track, and an upright cardboard positioned over the turntable's center. We utilized the Logitech C270 webcam, consistent with Kalaitzakis et al. [Kalaitzakis et al. 2021]. The webcam offers a camera stream resolution of 1280x720 at 25fps, featuring built-in auto white balance and lacking auto-focus functionality. We meticulously calibrated lens distortion and camera

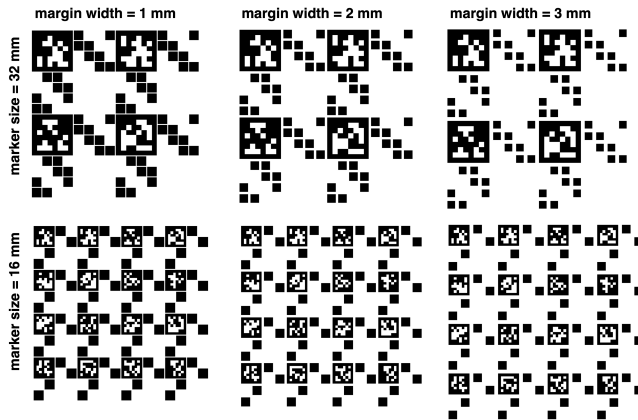


Figure 7: Increasing the margin width between visual components enhances the markers’ visibility but reduces the markers’ overall visual continuity.

perspective to align the camera’s center view with the cardboard’s center as it moved to a distance of d meters away and rotated to an angle of θ degrees towards the camera on the testing platform. The experiments were conducted in a daytime-lit room with diffusive curtains to ensure sufficient ambient light without the effects of direct sunlight.

We chose the original ArUco marker (Figure 8d) and AprilTag-36h10 marker (Figure 8e) for our evaluation because they have a comparable number of available IDs. The original ArUco markers (ArUco-original) have a 5x5 bit payload, providing 2048 unique IDs with a minimum Hamming distance of 3. The AprilTag-36h10 markers have a 6x6 bit payload, offering 2320 unique IDs with a minimum Hamming distance of 10. We used 16 markers with a width of s mm, ranging from ID=10 to ID=25, for testing. These markers were deployed in a four-by-four grid with a margin width of m mm and printed on paper with a laser printer.

We used the ArUco library implemented in OpenCV version 4.6.0.66 to recognize and track these two types of markers, *ArUco* and *AprilTag*. Through a pilot test, we determined three distances ($d = [0.5m, 0.75m, 1m]$), four rotation angles ($\theta = [0^\circ, 40^\circ, 60^\circ, 80^\circ]$), two marker sizes ($s = [16mm, 32mm]$), and three margin widths ($m = [1mm, 2mm, 3mm]$) for the two types of markers. For every case, 100 (frames) \times 16 (markers) = 1600 data points were collected for analysis.

Results. Figure 9 shows the marker *detection* results. In general, the detection rate was higher when the marker grid is facing the camera directly (i.e., $\theta = 0^\circ$) and tends to decrease as the marker grid is rotated (i.e., $\theta > 0^\circ$). The detection rate was higher with markers in a larger size (s) and a smaller distance (d) to the camera.

Regarding *ArUco* markers, when the marker grid rotation angle is $\theta \leq 40^\circ$, the $s = 32mm$ markers have a $> 95\%$ mean detection rate at $d = 1m$ and a $> 99\%$ mean detection rate at $d = 0.75m$. Similarly, the $s = 16mm$ markers have a $> 95\%$ mean detection rate at $d = 0.5m$ for all margin widths. However, when the rotation angle is $\theta = 60^\circ$, the ($s = 32mm, m = 1mm$) markers exhibit a noticeable decrease in the detection rate at both distances of $d = 0.75m$. In

contrast, the ($s = 32mm, m = 2mm$) and ($s = 32mm, m = 3mm$) markers can still sustain a $> 95\%$ mean detection rate. Similarly, both ($s = 32mm, m = 1mm$) and ($s = 32mm, m = 2mm$) markers exhibit a noticeable decrease in the detection rate at both distances of $d = 0.25m$ and $d = 0.5m$, whereas the ($s = 32mm, m = 3mm$) markers can still sustain a $> 95\%$ mean detection rate. Additionally, all conditions exhibit less than a $> 95\%$ mean detection rate at a rotation angle of $\theta = 80^\circ$.

AprilTag markers exhibit a smaller detection range than the *ArUco* markers due to their 6x6 payload resolution, which makes recognition harder over a distance compared to the 5x5 resolution of *ArUco* markers. When the marker grid rotation angle is $\theta \leq 40^\circ$, the $s = 32mm$ markers have a $> 95\%$ mean detection rate at a distance of $d = 0.75m$ for all margin widths. Similarly, the $s=16mm$ markers have a $> 95\%$ mean detection rate at a distance of $d = 0.5m$ when the margin width is $m = 3mm$, but they exhibit a reduced mean detection rate when $m = 2mm$ (94.75%) and $m=1$ (89.06%). When the rotation angle is $\theta = 60^\circ$, the $s = 32mm$ markers have a $> 95\%$ mean detection rate at a distance of $d = 0.5m$ for all margin widths. Additionally, no conditions exhibit a $> 95\%$ mean detection rate at a rotation angle of $\theta = 80^\circ$.

Figure 10 shows the marker *tracking* results. We select the test cases that achieved a detection rate of over 95% to further analyze the tracking performance by investigating their tracking data when the tags were detected.

We first identified that the detection sometimes returns an invalid tag rotation angle, which deviates by more than 90 degrees from the test case. We identify those invalid detections as *orientation tracking errors*. Figure 10a shows the mean correct orientation detection rate remains high when the tag rotation angle is $\theta = 0^\circ$ and decreases as the tag rotation angle increases. The effect is less significant with a wider margin width. Notably, the success rate of $s = 16mm, m = 3$ ArUco markers remains $> 95\%$ within a tag rotation angle of $\theta = 60$ degrees at a distance of $d = 0.5m$, and the success rate of $s = 32mm, m = 2$ for both ArUco and AprilTag markers remains $> 95\%$ within a tag rotation angle of $\theta = 40$ degrees at a distance of $d = 0.75m$.

Figure 10b shows the mean detected tag rotation angles in the correct orientation detection cases. Note that the standard deviations are higher when the rotation angle is smaller. All the test cases show comparable performances. Among all test cases at all distances and rotation angles, the median of mean errors is $Mdn = 1.53 \pm 0.64$ degrees with 3.59 degrees at maximum. Figure 10c also shows stable performance in mean detected tag distance to the camera, indicating overall tag localization performance when the tags were rotated. Among all test cases at all distances and rotation angles, the median of mean errors is $Mdn = 5.47 \pm 0.17cm$ with $8.06cm$ at maximum. Although results consist of a structural underestimation, the standard deviation is notably low. We see the structural underestimation of tag distances as artifacts due to the lens distortion correction after calibrating the camera. We consider this structural underestimation correctable, given that the detected tag distance is highly correlated to the actual distance. Overall, we observe promising tracking performance in the success cases.

3.3.2 Session 2. Margin Width vs. Marker Deformation. When wearing a piece of fabric, the way it bends can vary depending on the



Figure 8: Experimental apparatus: a) Apparatus for Session 1: 16mm-width markers with 1mm-width margin; b) Apparatus for Session 2: 16mm-width markers with 2mm-width margin deployed on a 4cm-radius cylinder; c) 32mm-width markers with 2mm-width margins deployed on an 8cm-radius cylinder; d) ArUco-original markers; e) AprilTag-36h10 markers.

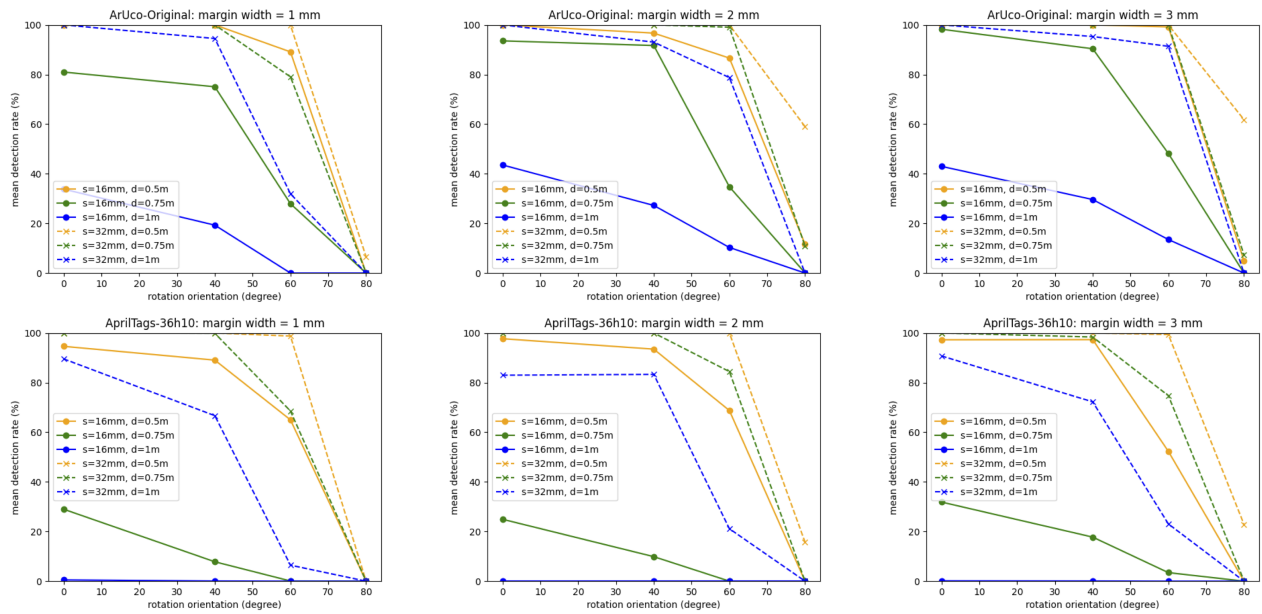


Figure 9: Marker detection results of Session 1. For both ArUco and AprilTag markers, a margin size of $m = 1\text{mm}$ proves sufficient when the grid rotation angle is small (i.e., $\theta \leq 40^\circ$). However, when the rotation angle is $\theta = 60^\circ$, the $m = 1\text{mm}$ markers exhibit a noticeable decrease in the detection rate at both distances, where the $m = 2\text{mm}$ and $m = 3\text{mm}$ markers can still sustain their mean detection rate.

body part it's worn on, influenced by factors like shape, movement, and pressure. These factors, in turn, are affected by the garment's fit, fabric type and elasticity, body movements, and specific body contours. In the case of loosely fitting clothes made of non-elastic fabrics, such as the Poncho depicted in Figure 1, the fabric drapes differently according to the contours of each body part. For instance, fabric over the shoulders may *bend* more than fabric over the hips and arms due to the unique shapes of these areas. Consequently, we conducted a study to assess the marker tracking performance across various bending radii.

Apparatus. Figure 8b depicts the experimental setup, comprising a C270 webcam and a track. We made three cylinders in a radius of $r = [4\text{cm}, 6\text{cm}, 8\text{cm}]$ to implement three surfaces of different

bending radii, allowing for mounting CV markers on the top for testing. We meticulously calibrated lens distortion and camera perspective to align the camera's center view with the center of the side of a cylinder as it moved to a distance of d m away from the camera, and the cylinder was not rotated (i.e., $\theta = 0^\circ$) during the test. The experiments were also conducted in a daytime-lit room with diffusive curtains to ensure sufficient ambient light without the effects of direct sunlight.

We chose the same set of ArUco and AprilTag markers and layouts as in Session 1 and used the same software to recognize and track these markers. Based on the findings of Session 1, we determined three distances ($d = [0.5\text{m}, 0.75\text{m}, 1\text{m}]$), three bending radius ($r = [4\text{cm}, 6\text{cm}, 8\text{cm}]$), one rotation angle ($\theta = 0^\circ$), two marker sizes ($s =$

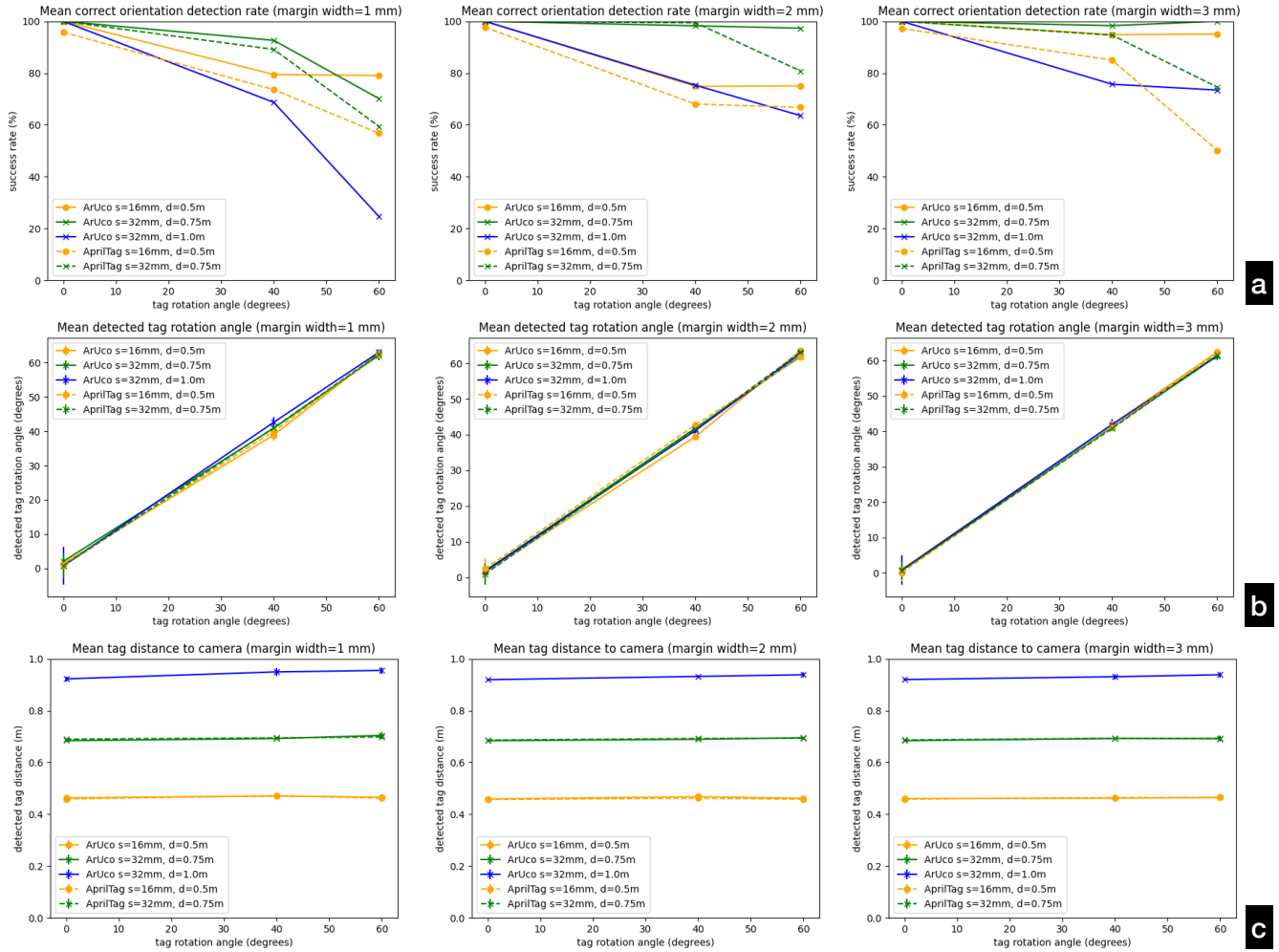


Figure 10: Marker tracking results of Session 1: a) the mean correct orientation detection rate remains high when the tag rotation angle is $\theta = 0^\circ$ and decreases as the tag rotation angle increases, but the effect is less significant with a wider margin width; b) mean detected tag rotation angles in the correct orientation detection cases; c) mean detected tag distance to the camera in the correct orientation detection cases.

[16mm, 32mm]), and three margin widths ($w = [1\text{mm}, 2\text{mm}, 3\text{mm}]$) for the two types of fiducial markers. For every case, 100 (frames) \times 16 (markers) = 1600 data points were collected for analysis.

Results. Figure 11 shows the overall marker *detection* results, and Figure 12 depicts the individual marker *tracking* results on selected cases. Similar to Session 1, we further identify the *successful* orientation tracking when the detected marker’s orientation deviates less than 90 degrees from its actual orientation, as the results shown in Figure 12a.

Regarding *ArUco* markers, when the bending radius is $r = 8\text{cm}$, the $s = 32\text{mm}$ markers have a $> 95\%$ mean detection rate at $d = 1\text{m}$ and a $> 99\%$ mean detection rate at $d = 0.75\text{m}$ for all margin widths. However, when the bending radius is $r = 6\text{cm}$, only the $s = 16\text{mm}$ markers achieved a $> 95\%$ mean detection rate at $d = 0.5\text{m}$ for all margin widths. Additionally, the $s = 16\text{mm}$ markers significantly

outperformed the $s = 32\text{mm}$ markers when the bending radius is $r = 4\text{cm}$. This is because the larger markers on the sides were not entirely visible when they were bent, as their lower tracking success rates shown in Figure 12a. When the bending radius is $r = 4\text{cm}$, the $s = 16\text{mm}, m = 2\text{mm}$ and $s = 16\text{mm}, m = 3\text{mm}$ markers’ tracking success rate on the sides were also affected, yet the performance decrease is less than $s = 16\text{mm}, m = 1\text{mm}$ ones.

Regarding *AprilTag* markers, when the bending radius is $r = 8\text{cm}$, both the $s = 16\text{mm}$ and $s = 32\text{mm}$ markers have a $> 95\%$ mean detection rate at $d = 0.5\text{m}$. However, when the bending radius is $r = 6\text{cm}$, only the $s = 16\text{mm}, m = 1\text{mm}$ markers achieved a $> 95\%$ mean detection rate at $d = 0.5\text{m}$ for all margin widths. Regarding the sides of markers when bent, *AprilTag* markers were less detectable than *ArUco* markers of the same size (i.e., $s = 16\text{mm}$), even with a larger margin size (i.e., $m = 3\text{mm}$), as shown in Figure 12a. Therefore, we

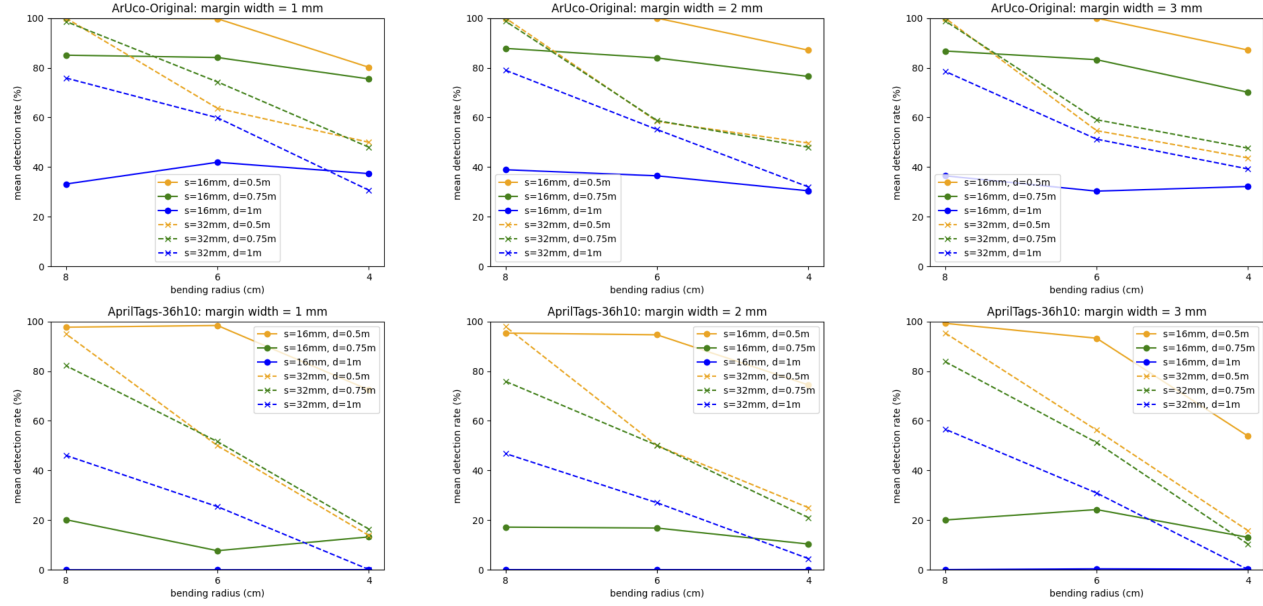


Figure 11: Marker detection results of Session 2. When the bending radius is $r = 6\text{cm}$, only the $s = 16\text{mm}$ markers sustain the mean detection rate at $d = 0.5\text{m}$ for all margin widths. Additionally, the $s = 16\text{mm}$ markers significantly outperformed the $s = 32\text{mm}$ markers when the bending radius is $r = 4\text{cm}$. This is because the larger markers on the sides were not entirely visible when bent.

believe the reduced performance is due to their higher (i.e., 6×6) payload resolution.

Figures 12b and 12c depict the individual marker tracking results for their mean rotation angle errors and distance errors when they were successfully detected at least once. In general, the results are comparable to those of Session 1 (Figure 10), and we did not observe a significant correlation between the marker bending and their tracking performance in our test cases, where the markers were uniformly bent on a cylinder at different bending radii.

3.3.3 Summary. Results from sessions 1 and 2 confirm the importance of selecting an appropriate margin width to ensure uncompromised marker tracking performance. For both ArUco and AprilTag markers chosen for our study, a margin size of $m = 1\text{mm}$ proves sufficient for detection, and $m = 2\text{mm}$ proves sufficient for tracking when the grid rotation angle is small (i.e., $\theta \leq 40^\circ$) and deformation is minimal (i.e., $r = 8\text{cm}$). This applies generally to the $s = 16\text{mm}$ ArUco markers and the $s = 32\text{mm}$ AprilTag markers at a tracking distance of 0.5m and the $s = 32\text{mm}$ ArUco markers at a 0.75m tracking distance. For tracking on curved surfaces or longer distances, markers with lower-resolution payloads (e.g., ArUco-Original) performed better than the ones with higher-resolution payloads (e.g., AprilTag-36h10). Designers can opt for larger markers to cover larger garment pieces (**P2**) or smaller markers to accommodate deformation better over the shoulders and arms.

Considering the optimization of object identification and tracking (**P1**), we do not recommend further reducing the margin size, as this would limit tracking orientation range and reliability. Increasing the margin size between markers can increase tracking performance slightly, yet increasing the margin beyond necessity

may impact aesthetics (**P3**). As only the margin surrounding the fiducial markers is necessary, designers can merge the small decorators in Figure 6c and increase the N value of the Pied-de-poule pattern to increase the visual continuity (**P3**), as shown in Figure 5.

3.4 Sublimation Printing Fiducial Markers on Fabrics

Printing fiducial markers through sublimation printing in the garment design is easier than traditional methods such as knitting and weaving. Sublimation printing allows users to fabricate digital patterns on existing fabric structures by heat-transferring dye onto them. The process involves printing designs onto special sublimation paper using dye-based inks and then using heat and pressure to transfer the ink onto the material. When heated, the ink turns into a gas without passing through a liquid phase, bonding directly with the material's fibers. This results in vibrant, long-lasting prints with excellent color reproduction and durability.

3.4.1 Generating Fiducial Marker Patterns. We developed a Chic-Marker Generator, a Python script that integrates OpenCV's marker generation capability and the Pied-de-poule generation algorithm of Feijis [Feijis 2012]. The script facilitates users in generating a marker pattern with specified parameters, including marker type (e.g., `-type "AprilTag36h11"`), marker size (e.g., `-size 32` for $s = 32\text{mm}$), margin width (e.g., `-margin 1` for $m = 32\text{mm}$), grid size (e.g., `-gridx 16 -gridy 16` for a 16×16 grid), and pattern type (e.g., `-n 2 -version DECOR` for an $N=2$ Pied-de-poule pattern with decorators). Subsequently, users save the output as a PNG file in specific resolution and real-world size (e.g., `-dpi 72 -sheet A3`

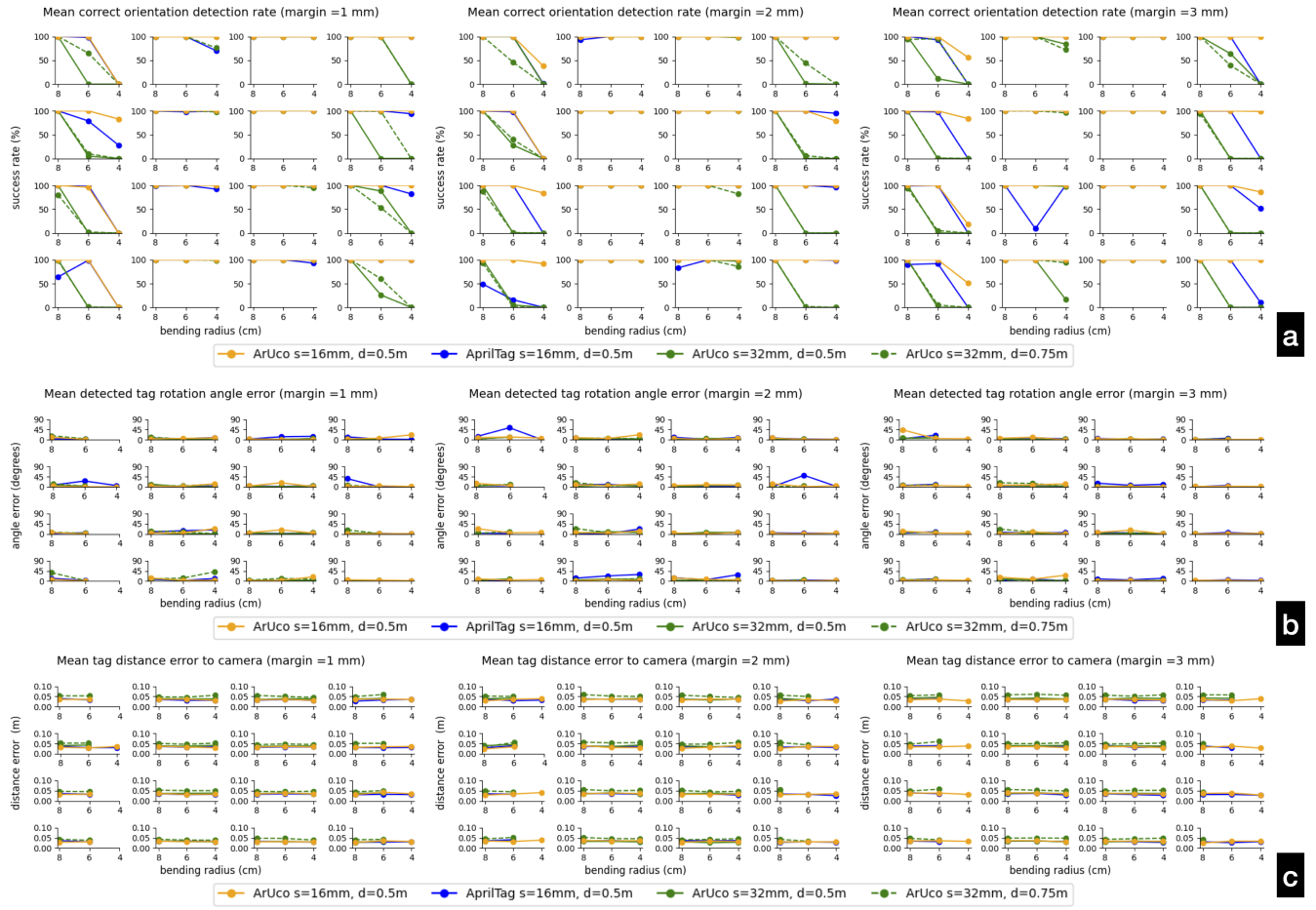


Figure 12: Individual marker tracking results of Session 2: a) the mean correct orientation detection rates when the markers were bent in different radii; b) mean detected tag rotation errors in the correct orientation detection cases; c) mean detected tag distance errors to the camera in the correct orientation detection cases.

for a 72-DPI print on an A3 sheet). The output patterns can then be imported into design software for further editing, printed on sublimation paper using an inkjet printer with sublimation ink, and transferred onto fabrics with heat.

3.4.2 Fabric Materials for Printing Fiducial Markers. Polyester fabrics are well-suited for sublimation printing due to their chemical composition and physical properties. They are made from synthetic fibers with a high affinity for sublimation dyes. When exposed to heat and pressure during the sublimation printing process, the polyester fibers open up and allow the dye molecules to penetrate deeply into the fabric. This results in vibrant and long-lasting colors embedded within the fabric rather than on the surface.

Figure 13 depicts samples subjected to sublimation printing and their 200 \times magnified view, where 38mm- and 8mm-width AprilTag-36h11 markers are printed on each sample with a 2mm-width margin in a N=2 Pied-de-poule pattern. We tested the fiducial patterns on a variety of polyester fabrics, including satin-woven polyester fabrics (Figures 13a, 13b, and 13c) characterized by a smooth and

shiny surface, plain-woven polyester fabrics (Figures 13d and 13e) that are the most common and less shiny than satin-woven ones, blackout polyester fabrics (Figures 13a and 13d) that prevent light penetration, as well as knitted polyester (Figure 13f) and combined cotton and elastane woven polyester (Figure 13g) fabrics that are stretchable and skin-friendly. Regarding baseline conditions, we also tested the fiducial patterns on plain-woven cotton fabrics that underwent rub treatment (Figure 13h) and were combined with linen (Figure 13i), resulting in increased moisture absorption and better wrinkle resistance. As a result, all the polyester fabrics yield significantly better printing results than cotton and combined cotton and elastane woven polyester fabrics. With sufficient ambient light, the experimental apparatus can identify all 8mm-width markers on the satin-woven and plain-woven polyester fabrics at a close-up distance. Blackout polyester fabrics have a light-blocking layer sandwiched between the top and bottom layers, providing better visual contrasts than the non-blackout ones.

Through hands-on exploration, we also excluded a few options. The front side of satin-woven polyester fabrics has a smooth and

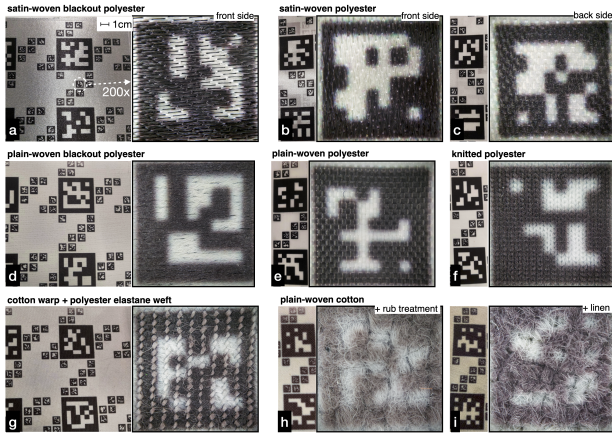


Figure 13: Sublimation printing material exploration. All the polyester fabrics yield significantly better printing results than cotton and combined cotton and elastane woven polyester fabrics. Blackout polyester fabrics, which have a light-blocking layer sandwiched in between the top and bottom layers, provide better visual contrasts than the non-blackout ones.

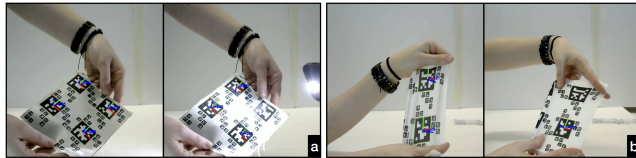


Figure 14: Failure cases during hands-on explorations: a) The front side of satin-woven polyester fabrics is more reflective to directional light or spotlight, failing marker detection; b) Stretchable fabrics such as knitted polyester also confuse the marker detection algorithm when under tension, leading to failure in marker recognition and imprecise pose tracking.

shiny surface, which is more reflective to directional light or spotlight, failing marker detection, as shown in Figure 14a. Stretchable fabrics such as knitted polyester also confuse the marker detection algorithm when under tension, leading to failure in marker recognition and imprecise pose tracking, as shown in Figure 14b.

3.4.3 Summary. We recommend sublimation printing fiducial markers on plain-woven, non-stretchable polyester fabrics. A blackout layer in the middle is preferred in applications where light blocking is desired. Satin-woven polyester fabrics are also suitable when printed on the backside, which is less smooth and shiny if plain-woven fabrics are unavailable.

4 EXPLORATORY MAKING

In this section, we delve deeper into the design opportunities and uncover hidden technical issues of Chic-Marker through a series of exploratory making [Zimmerman et al. 2007].

4.1 Interdisciplinary Co-creation

Process. The process depicted in Figure 3 also illustrates a three-hour session where two co-authors collaborated in making, one with two decades of programming experience and the other with more than 18 years of professional fashion design experience. They commenced with a brief 15-minute discussion, following which one author generated patterns for sublimation printing while the other prepared files for laser-cutting polyester fabric. Together, they transferred the sublimation printed patterns onto the laser-cut polyester fabric. Subsequently, the fashion designer independently completed the making process over the next 90 minutes.

Results. The co-creation session resulted in four proof-of-concept apparel and accessories, including a tube dress, a sleeveless jogging shirt, a reusable shopping bag, and a handbag, as depicted in Figure 2. All four items utilized the backside of satin-woven polyester fabrics for sublimation printing. Both the tube dress and sleeveless jogging shirt featured an N=2 Pied-de-poule design with AprilTag-36h11 markers sized at $s = 34\text{mm}$ and square decorators with a width of 8mm, along with a margin width of $m = 2\text{mm}$. The reusable shopping bag employed a puppy tooth (N=1 Pied-de-poule) design with AprilTag-36h11 markers sized at $s = 34\text{mm}$ and $s = 16\text{mm}$, also with a margin of $m = 2\text{mm}$. The handbag utilized an N=2 Pied-de-poule design with AprilTag-36h11 markers sized at $s = 19\text{mm}$ and square decorators with a width of 4mm, along with a margin width of $m = 1\text{mm}$.

Through an informal test conducted using our experimental apparatus and the procedure introduced in Study 1, the results demonstrated that markers sized at $s = 34\text{mm}$, $s = 19\text{mm}$, and $s = 16\text{mm}$ support tracking distances of more than 1m, 0.5m, and 0.5m, respectively, with a rotation angle of $\theta = 0^\circ$ when laid flat, thus affirming the validity of sublimation printing.

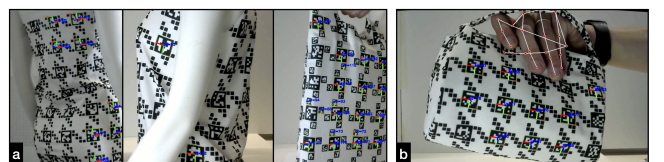


Figure 15: Challenging scenarios for fiducial marker tracking: a) fabric deformation and occlusion by body parts; b) utilizing pre-trained human hand and body models can offer contextual insights on marker occlusion and object usage.

Challenges and Opportunities. Figure 15a illustrates challenging cases for fiducial marker tracking, such as deformation and occlusion by body parts, which are common in garment and body-centric applications. To further reduce wrinkling and improve the garment's fit to the user's body, we recommend fabric shaping techniques that minimize wrinkles, such as darting and seam shaping. When combined with textile flattening methods like underlining, interfacing, and blocking, these techniques can enhance the garment's fit without compromising the detection rate. Experienced designers can also utilize draping techniques to prevent wrinkles. However, We advise against using folding and gathering techniques such

as pleating, shirring, and ruching, as they likely introduce more wrinkles into the fabric.

From a system's perspective, utilizing a pre-trained model for human hand and body tracking, implemented using Google MediPipe¹, can provide contextual insights on marker occlusion and object usage, as shown in Figure 15b.

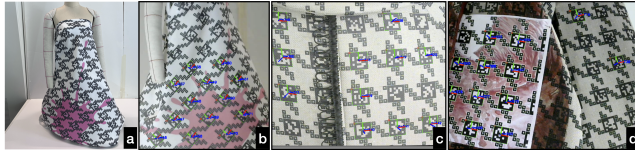


Figure 16: Patterns with overlaid graphics: a) a dress with pink splash graphics, meticulously designed to minimize interference with fiducial marker tracking; b) under ambient light conditions, undistorted markers function fully; c) redundant markers surrounding the red herring enable recognition and tracking of the garment; d) adding a white outline and solid fill in the payload to facilitating detection of markers positioned in front of the red herring.

4.2 Integrating Graphical Elements into Marker Patterns

Deviating from the guideline to optimize aesthetics is desirable as long as it does not impact the tracking performance significantly. Figure 16a displays a dress overlaid with pink splash graphics, meticulously designed to minimize interference with fiducial marker tracking. The light pink color was selected considering the default marker detection algorithm in OpenCV, which converts every pixel in the *RGB* color camera stream into the grayscale channel *Y* using the formula $Y = 0.299R + 0.587G + 0.114B$, often interpreting the light pink color as white. The contour of the splash was carefully arranged to avoid intersecting with the payload, reducing errors in payload decoding. A slightly lighter pink color is used inside the marker than outside, ensuring the color difference remains imperceptible to human eyes. Under ambient light conditions, undistorted markers function fully, as depicted in Figure 16b.

The *Red Herring* garment depicted in Figure 1 priorizes aesthetic expression, so our focus is not on ensuring the detection of all markers but rather on preserving the integrity of visual design. The redundant markers surrounding the red herring enable recognition and tracking of the garment, as shown in Figure 16c. Figure 16d presents an alternative design that maximizes marker detectability by adding a white outline and solid fill in the payload, facilitating the detection of markers positioned in front of the red herring.

Guidelines. Through the exploration, we derive two guidelines for adding a visual overlay that maintains the detectability of the markers. First, the overlaying graphics should not disrupt the adaptive thresholding and the payload decoding. The shading should prefer a solid or smooth gradient fill over a texture of dots and lines, especially in the marker's payload region and at corners. Second, the color of markers can deviate from black and white. Still, it

¹<https://developers.google.com/mediapipe>

should use the color most likely translated as the intended black and white color after grayscale operation and thresholding, such as applying dark green for black and light purple for white. The designer can further adjust the tone and brightness of the color for harmonization but should be mindful that a lenient color choice requires stricter environmental lighting requirements.

4.3 Long-Distance Marker Tracking

Long-distance marker tracking is crucial for various applications where precise localization over extended ranges is essential for navigation and monitoring in fields like robotics, augmented reality, and vitality, as well as for applications like detecting and tracking objects or individuals across expansive areas, enhancing security and situational awareness.

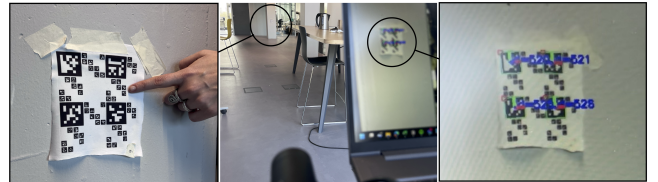


Figure 17: Four 38mm-width markers printed on polyester fabrics were successfully detected by a camera using 10x optical zoom from a distance of 12 meters.

Figure 17 depicts a sample with four 38mm-width markers printed on polyester fabrics, which can be detected by a streaming camera with an add-on lens that supports 10x optical zoom from a distance of 12 meters. Applying these patterns to the human body can leverage the auto-focusing features to make long-range motion tracking technically feasible. However, as users may not easily discern whether the camera is active, such a system must comply with ethical and privacy regulations to ensure user acceptance.

5 DISCUSSION

Fashion Technology Designers Need Low-Threshold Toolkits. Fashion technology aims to harmonize human-computer interactions (HCI) with a wearer's aesthetic, expressive, and social needs [Tomico et al. 2017]. There has been a recent push to integrate the aesthetic appeal of products, making them more desirable [Pan and Stolterman 2015]. The appearance and expressiveness of these products are crucial as they serve as an interface between our bodies and society [Berzowska 2005; Tomico et al. 2017]. Moreover, they enable the everyday expression of identity and personal values, and facilitate social connections [Crane 2000; Pan and Stolterman 2015]. Although numerous electronic toolkits and techniques have enabled aesthetic expressions with interactivity [Berzowska and Coelho 2005; Freire et al. 2017; Kao et al. 2016], many fashion designers skilled in machinery operation and handcrafting lack experience in using digital technologies involving electronics and programming [Seyed et al. 2021]. Therefore, having a low-threshold toolkit that integrates seamlessly with the designer's existing workflow is crucial for further exploration.

Accessible Fabrication Workflow. The Chic-Marker approach presented in this study seamlessly integrates with the designer's existing garment-making workflow (Figure 3). Once the fiducial marker patterns are generated as a file, the designer can easily apply the pattern within their design software and print it onto sublimation ink-transfer paper. The designers test the locations between the shape of the garment panels and the marker location on their graphic design software (e.g., Adobe Illustrator) before deciding on the laser-cutting pattern. They can use image processing software (e.g., Adobe Photoshop) already in their workflow to adjust the intensity and location of the graphic overlay to ensure they do not interfere with marker tracking. They also marked reference points to facilitate the physical alignment between the sublimation transfer paper and the laser-cut fabrics to ensure the final results. Future work can eliminate this alignment effort by enabling users to directly laser cut the fabrics with the markers sublimation printed.

In addition to sublimation printing, the process and results described can be replicated using conventional hand tools. The heat-transfer process can be carried out using irons or a heat presser. Laser-cutting can be achieved with scissors, and sewing can be done by hand instead of a sewing machine. This accessible workflow empowers fashion designers to unleash their creativity in fabricating apparel and accessories adorned with fiducial markers.

Applications, Benefits, and Scale. When the users have the agency in camera use and are willing to be monitored by a camera to increase their HCI efficiency, such as enhancing human-robot interactions, in-door localization, monitoring their fitness or exercise performances, and gaming in mixed reality, using the fiducial markers potentially improve the user experiences in these applications. The camera tracks the markers precisely without requiring end-user calibrations. Furthermore, when worn outside the range of a camera, the marker-equipped wearable remains inconspicuous and aesthetically pleasing.

Motion tracking applications require each marker to be unique to maintain a one-to-one relationship between each marker and its corresponding location. Our work uses the April36h10 (6×6 payload, Hamming distance = 10) markers and ArUco-Original markers (5×5 payload, Hamming distance = 3), which both provide more than 2000 unique IDs for making body-size garments. Industries that need to scale up production to manufacture a larger number of unique pieces or a larger piece of garment (e.g., for furniture) can consider adapting the patterns to an alternative AprilTag family that also uses the outside of squares for decoding the bits (e.g., AprilTag-Standard52h13², which provides 48,714 unique IDs) or build a customized tag family with a smaller Hamming distance to provide more IDs without increasing the resolution of the payload to sustain marker tracking performance.

Privacy and Data Regulation. Using webcams or surveillance cameras to track wearables in human-centered applications may pose risks and privacy concerns [Hong and Landay 2004]. When the users do not have complete control of the camera and the data generated, wearing fiducial markers may raise privacy concerns because the markers enable a camera system to track individuals' movements without consent. Especially in healthcare settings,

ensuring informed consent and individuals understand the implications and control the data collection. Regulations, such as The EU Artificial Intelligence Act³, are necessary to prevent misuse of these collected data in social scoring, identification, or categorization.

Marker-based Approaches vs. Markerless Approaches. The proposed system extends current motion-capturing suits (e.g., [Chen et al. 2021]) or green-screen dresses (e.g., Mackey et al. [Mackey et al. 2020]) by enabling garment tracking while maintaining aesthetic appeal for everyday wear. The marker tracking results include multiple markers' IDs and their six degrees of freedom information, measured in real-world units (e.g., cm), which remains a challenge for markerless approaches [Fan et al. 2022], even for rigid-body objects. Therefore, in alignment with Chen et al. [Chen et al. 2021], we argue that our marker-based approach is more practical for garments, especially when they are mildly deformed. Future work could also leverage deep learning techniques such as Deep ChArUco [Hu et al. 2019] to enhance the capability of handling low-light, high-motion, and high-blur scenarios, which are common in tracking moving human subjects in real-world settings.

User Interfaces. The pattern generator is currently made as a command-line tool, as described in Section 3.4.1. The Python script for generating fiducial marker patterns was effective in facilitating multidisciplinary collaboration, but it was not specifically designed for novice users. We have addressed this by incorporating a graphical user interface that allows users to adjust marker sizes and margin widths and preview the results in real-time. However, the gap between the layout of markers and their actual placement on garments remains open. Additionally, understanding the implications of marker size and density on recognition and tracking distance becomes more intuitive when considering aesthetic design considerations. Future efforts could focus on providing a more integrated software interface to offer designers a better overview, facilitating independent exploration.

Limitations and Future Work. Pied-de-poule is not just a visual pattern but is also associated with material texture. It is traditionally done with woven patterns and thick yarn. Our work used the visual pattern of pied-de-poule but not the woven structure. Future research could be done on the woven structure with different yarn colors for further integration.

Our work enables a fashionable design for the fiducial marker-embedded garments. Based on the presented technique, future work can further evaluate with users to understand the designs' acceptance and address the users' willingness to adopt this marker-enhanced fashion. User studies could facilitate an understanding of how perception could strengthen practical applications by conducting user studies to assess social acceptance and practical usability in everyday scenarios. In the extended period of use, the tracking purpose of visible markers is recognized and noticed by others and may lead to undesirable impressions. The uncertain long-term effects on social acceptance necessitate further investigation.

²<https://github.com/AprilRobotics/apriltag>

³<https://artificialintelligenceact.eu/>

6 CONCLUSION

In recent years, fashion technology has expanded into various domains, including smart textiles, augmented reality fashion, and sustainable fashion practices. Wearable technology involves integrating electronic devices and sensors into garments or accessories to enhance performance and provide interactive experiences. Non-electronic solutions, such as fiducial markers, are more sustainable but harder to conceal.

Our research proposes a novel approach that integrates the square fiducial markers into timeless Pied-de-poule patterns so they can be stylishly integrated into apparel and accessories. By not concealing these square fiducial markers, a conventional color camera can recognize and track them in the real world, providing an additional digital layer of information related to the garments and their owners. Through technical evaluation and exploratory making, we have provided guidelines regarding the primary considerations of optimizing object identification and tracking, efficient use of IDs, and balancing aesthetics and performance. We have also presented a workflow based on sublimation printing to achieve these results.

We hope this method will help push the boundaries of fashion technology in augmented reality, offering new avenues for creativity, personalization, and connectivity within the ever-evolving landscape of fashion and consumer culture.

ACKNOWLEDGMENTS

We would like to express our gratitude to the anonymous reviewers for their valuable input. Special thanks go to Brun Stöver, Femke Vorselen, Feije van de Wetering, and Deniz Korkmaz for their assistance during the development and to the staff and students in the Crafting Wearable Senses squad and Fashion Tech Farm for their feedback throughout the project.

REFERENCES

- Filippo Bergamasco, Andrea Albarelli, Luca Cosmo, Emanuele Rodolà, and Andrea Torsello. 2016. An Accurate and Robust Artificial Marker Based on Cyclic Codes. *IEEE Transactions on Pattern Analysis and Machine Intelligence* 38, 12 (2016), 2359–2373. <https://doi.org/10.1109/TPAMI.2016.2519024>
- Filippo Bergamasco, Andrea Albarelli, Emanuele Rodolà, and Andrea Torsello. 2011. RUNE-Tag: A high accuracy fiducial marker with strong occlusion resilience. In *CVPR 2011*. 113–120. <https://doi.org/10.1109/CVPR.2011.5995544>
- Joanna Berzowska. 2005. Electronic textiles: Wearable computers, reactive fashion, and soft computation. *Textile* 3, 1 (2005), 58–75.
- Joanna Berzowska and Marcelo Coelho. 2005. Kukkia and vilkas: Kinetic electronic garments. In *Ninth IEEE international symposium on wearable computers (ISWC'05)*. IEEE, 82–85.
- Mark Billinghurst, Hirokazu Kato, and Ivan Poupyrev. 2001. The magicbook-moving seamlessly between reality and virtuality. *IEEE Computer Graphics and Applications* 21, 3 (2001), 6–8.
- Lilian Calvet, Pierre Gurdjos, Carsten Griwodz, and Simone Gasparini. 2016. Detection and Accurate Localization of Circular Fiducials under Highly Challenging Conditions. In *2016 IEEE Conference on Computer Vision and Pattern Recognition (CVPR)*. 562–570. <https://doi.org/10.1109/CVPR.2016.67>
- He Chen, Hyojoon Park, Kutay Macit, and Ladislav Kavan. 2021. Capturing detailed deformations of moving human bodies. *ACM Trans. Graph.* 40, 4, Article 85 (jul 2021), 18 pages. <https://doi.org/10.1145/3450626.3459792>
- Diana Crane. 2000. *Fashion and its social agendas: Class, gender, and identity in clothing*. University of Chicago Press.
- Joseph DeGol, Timothy Bretl, and Derek Hoiem. 2017. Chromatag: A colored marker and fast detection algorithm. In *Proceedings of the IEEE International Conference on Computer Vision*. 1472–1481.
- Mustafa Doga Dogan, Raul Garcia-Martin, Patrick William Haertel, Jamison John O'Keefe, Ahmad Taka, Akash Aurora, Raul Sanchez-Reillo, and Stefanie Mueller. 2023. BrightMarker: 3D Printed Fluorescent Markers for Object Tracking. In *Proceedings of the 36th Annual ACM Symposium on User Interface Software and Technology* (San Francisco, CA, USA) (*UIST '23*). Association for Computing Machinery, New York, NY, USA, Article 55, 13 pages. <https://doi.org/10.1145/3586183.3606758>
- Mustafa Doga Dogan, Ahmad Taka, Michael Lu, Yunyi Zhu, Akshat Kumar, Akar Gupta, and Stefanie Mueller. 2022. InfraredTags: Embedding Invisible AR Markers and Barcodes Using Low-Cost, Infrared-Based 3D Printing and Imaging Tools. In *Proceedings of the 2022 CHI Conference on Human Factors in Computing Systems* (New Orleans, LA, USA) (*CHI '22*). Association for Computing Machinery, New York, NY, USA, Article 269, 12 pages. <https://doi.org/10.1145/3491102.3501951>
- Zhaoxin Fan, Yazhi Zhu, Yulin He, Qi Sun, Hongyan Liu, and Jun He. 2022. Deep learning on monocular object pose detection and tracking: A comprehensive overview. *Comput. Surveys* 55, 4 (2022), 1–40.
- Loe MG Feijis. 2012. Geometry and Computation of Houndstooth (Pied-de-poule). In *Proceedings of Bridges 2012: Mathematics, Music, Art, Architecture, Culture*. 299–306.
- Mark Fiala. 2005. ARTag, a fiducial marker system using digital techniques. In *2005 IEEE Computer Society Conference on Computer Vision and Pattern Recognition (CVPR'05)*, Vol. 2. IEEE, 590–596.
- Mark Fiala. 2009. Designing highly reliable fiducial markers. *IEEE Transactions on Pattern analysis and machine intelligence* 32, 7 (2009), 1317–1324.
- Karin Margarita Frei. 2009. News on the geographical origin of the Gerum cloak's raw material. *Fornvännen* 104, 4 (2009), 313–315.
- Rachel Freire, Cedric Honnet, and Paul Strohmeier. 2017. Second skin: An exploration of etextile stretch circuits on the body. In *Proceedings of the Eleventh International Conference on Tangible, Embedded, and Embodied Interaction*. 653–658.
- Jorge Fuentes-Pacheco, José Ruiz-Ascencio, and Juan Manuel Rendón-Mancha. 2015. Visual simultaneous localization and mapping: a survey. *Artificial intelligence review* 43 (2015), 55–81.
- Sergio Garrido-Jurado, Rafael Muñoz-Salinas, Francisco José Madrid-Cuevas, and Manuel Jesús Marín-Jiménez. 2014. Automatic generation and detection of highly reliable fiducial markers under occlusion. *Pattern Recognition* 47, 6 (2014), 2280–2292.
- Christopher Getschmann and Florian Echtler. 2021. Seedmarkers: Embeddable Markers for Physical Objects. In *Proceedings of the Fifteenth International Conference on Tangible, Embedded, and Embodied Interaction* (Salzburg, Austria) (*TEI '21*). Association for Computing Machinery, New York, NY, USA, Article 26, 11 pages. <https://doi.org/10.1145/3430524.3440645>
- Jonna Häkkilä, Ashley Colley, Paula Roinesalo, and Jani Väyrynen. 2017. Clothing integrated augmented reality markers. In *Proceedings of the 16th International Conference on Mobile and Ubiquitous Multimedia* (Stuttgart, Germany) (*MUM '17*). Association for Computing Machinery, New York, NY, USA, 113–121. <https://doi.org/10.1145/3152832.3152850>
- Jason I. Hong and James A. Landay. 2004. An architecture for privacy-sensitive ubiquitous computing. In *Proceedings of the 2nd International Conference on Mobile Systems, Applications, and Services* (Boston, MA, USA) (*MobiSys '04*). Association for Computing Machinery, New York, NY, USA, 177–189. <https://doi.org/10.1145/990064.990087>
- Danying Hu, Daniel DeTone, and Tomasz Malisiewicz. 2019. Deep charuco: Dark charuco marker pose estimation. In *Proceedings of the IEEE/CVF Conference on computer vision and pattern recognition*. 8436–8444.
- Michail Kalaitzakis, Brennan Cain, Sabrina Carroll, Anand Ambrosi, Camden Whitehead, and Nikolaos Vitzilaios. 2021. Fiducial markers for pose estimation: Overview, applications and experimental comparison of the arttag, apriltag, aruco and stag markers. *Journal of Intelligent & Robotic Systems* 101 (2021), 1–26.
- Martin Kaltenbrunner and Ross Bencina. 2007. reacTIVision: a computer-vision framework for table-based tangible interaction. In *Proceedings of the 1st International Conference on Tangible and Embedded Interaction* (Baton Rouge, Louisiana) (*TEI '07*). Association for Computing Machinery, New York, NY, USA, 69–74. <https://doi.org/10.1145/1226969.1226983>
- Hsin-Liu Kao, Christian Holz, Asta Roseway, Andres Calvo, and Chris Schmandt. 2016. DuoSkin: rapidly prototyping on-skin user interfaces using skin-friendly materials. In *Proceedings of the 2016 ACM International Symposium on Wearable Computers*. 16–23.
- Han-Jong Kim, Ju-Whan Kim, and Tek-Jin Nam. 2016. miniStudio: Designers' Tool for Prototyping Ubicomp Space with Interactive Miniature. In *Proceedings of the 2016 CHI Conference on Human Factors in Computing Systems* (San Jose, California, USA) (*CHI '16*). Association for Computing Machinery, New York, NY, USA, 213–224. <https://doi.org/10.1145/2858036.2858180>
- Dingzeyu Li, Avinash S. Nair, Shree K. Nayar, and Changxi Zheng. 2017. AirCode: Unobtrusive Physical Tags for Digital Fabrication. In *Proceedings of the 30th Annual ACM Symposium on User Interface Software and Technology* (Québec City, QC, Canada) (*UIST '17*). Association for Computing Machinery, New York, NY, USA, 449–460. <https://doi.org/10.1145/3126594.3126635>
- David G Lowe. 2004. Distinctive image features from scale-invariant keypoints. *International journal of computer vision* 60 (2004), 91–110.
- Angella Mackey, Ron Walkary, Stephan Wensveen, Annika Hupfeld, and Oscar Tomico. 2020. Alternative Presents for Dynamic Fabric. In *Proceedings of the 2020 ACM Designing Interactive Systems Conference* (Eindhoven, Netherlands) (*DIS '20*). Association for Computing Machinery, New York, NY, USA, 351–364. <https://doi.org/10.1145/3357236.3395447>

- Kaj Mäkelä, Sara Belt, Dan Greenblatt, and Jonna Häkkilä. 2007. Mobile interaction with visual and RFID tags: a field study on user perceptions. In *Proceedings of the SIGCHI Conference on Human Factors in Computing Systems* (San Jose, California, USA) (*CHI '07*). Association for Computing Machinery, New York, NY, USA, 991–994. <https://doi.org/10.1145/1240624.1240774>
- L. Naimark and E. Foxlin. 2002. Circular data matrix fiducial system and robust image processing for a wearable vision-inertial self-tracker. In *Proceedings. International Symposium on Mixed and Augmented Reality*. 27–36. <https://doi.org/10.1109/ISMAR.2002.1115065>
- Edwin Olson. 2011. AprilTag: A robust and flexible visual fiducial system. In *2011 IEEE international conference on robotics and automation*. IEEE, 3400–3407.
- Yue Pan and Erik Stoltzman. 2015. What if HCI becomes a fashion driven discipline?. In *Proceedings of the 33rd annual ACM conference on human factors in computing systems*. 2565–2568.
- Francisco J Romero-Ramirez, Rafael Muñoz-Salinas, and Rafael Medina-Carnicer. 2018. Speeded up detection of squared fiducial markers. *Image and vision Computing* 76 (2018), 38–47.
- Mohammad Fattah Sani and Ghader Karimian. 2017. Automatic navigation and landing of an indoor AR, drone quadrotor using ArUco marker and inertial sensors. In *2017 international conference on computer and drone applications (ICoDA)*. IEEE, 102–107.
- Teddy Seyed, James Devine, Joe Finney, Michal Moskal, Peli de Halleux, Steve Hodges, Thomas Ball, and Asta Roseway. 2021. Rethinking the Runway: Using Avant-Garde Fashion To Design a System for Wearables. In *Proceedings of the 2021 CHI Conference on Human Factors in Computing Systems* (Yokohama, Japan) (*CHI '21*). Association for Computing Machinery, New York, NY, USA, Article 45, 15 pages. <https://doi.org/10.1145/3411764.3445643>
- Yuta Sugiura, Daisuke Sakamoto, Anusha Withana, Masahiko Inami, and Takeo Igarashi. 2010. Cooking with robots: designing a household system working in open environments. In *Proceedings of the SIGCHI Conference on Human Factors in Computing Systems* (Atlanta, Georgia, USA) (*CHI '10*). Association for Computing Machinery, New York, NY, USA, 2427–2430. <https://doi.org/10.1145/1753326.1753693>
- Oscar Tomico, Lars Hallnäs, Rung-Huei Liang, and Stephan AG Wensveen. 2017. Towards a next wave of wearable and fashionable interactions. *International Journal of Design* 11, 3 (2017).
- John Wang and Edwin Olson. 2016. AprilTag 2: Efficient and robust fiducial detection. In *2016 IEEE/RSJ International Conference on Intelligent Robots and Systems (IROS)*. IEEE, 4193–4198.
- Roy Want, Kenneth P. Fishkin, Anuj Gujar, and Beverly L. Harrison. 1999. Bridging physical and virtual worlds with electronic tags. In *Proceedings of the SIGCHI Conference on Human Factors in Computing Systems* (Pittsburgh, Pennsylvania, USA) (*CHI '99*). Association for Computing Machinery, New York, NY, USA, 370–377. <https://doi.org/10.1145/302979.303111>
- Karl D. D. Willis, Takaaki Shiratori, and Moshe Mahler. 2013. HideOut: mobile projector interaction with tangible objects and surfaces. In *Proceedings of the 7th International Conference on Tangible, Embedded and Embodied Interaction* (Barcelona, Spain) (*TEI '13*). Association for Computing Machinery, New York, NY, USA, 331–338. <https://doi.org/10.1145/2460625.2460682>
- Karl D. D. Willis and Andrew D. Wilson. 2013. InfraStructs: fabricating information inside physical objects for imaging in the terahertz region. *ACM Trans. Graph.* 32, 4, Article 138 (jul 2013), 10 pages. <https://doi.org/10.1145/2461912.2461936>
- Po-Chen Wu, Robert Wang, Kenrick Kin, Christopher Twigg, Shangchen Han, Ming-Hsuan Yang, and Shao-Yi Chien. 2017. DodecaPen: Accurate 6DoF Tracking of a Passive Stylus. In *Proceedings of the 30th Annual ACM Symposium on User Interface Software and Technology* (Québec City, QC, Canada) (*UIST '17*). Association for Computing Machinery, New York, NY, USA, 365–374. <https://doi.org/10.1145/3126594.3126664>
- Jamie Wubben, Francisco Fabra, Carlos T Calafate, Tomasz Krzeszowski, Johann M Marquez-Barja, Juan-Carlos Cano, and Pietro Manzoni. 2019. Accurate landing of unmanned aerial vehicles using ground pattern recognition. *Electronics* 8, 12 (2019), 1532.
- Guoxing Yu, Yongtao Hu, and Jingwen Dai. 2020. TopoTag: A robust and scalable topological fiducial marker system. *IEEE Transactions on Visualization and Computer Graphics* 27, 9 (2020), 3769–3780.
- John Zimmerman, Jodi Forlizzi, and Shelley Evenson. 2007. Research through design as a method for interaction design research in HCI. In *Proceedings of the SIGCHI Conference on Human Factors in Computing Systems* (San Jose, California, USA) (*CHI '07*). Association for Computing Machinery, New York, NY, USA, 493–502. <https://doi.org/10.1145/1240624.1240704>